THERMAL EVOLUTION OF LUNAR FELDSPATHIC BRECCIAS CONSTRAINED BY ^{40}AR/^{39}AR THERMOCHRONOLOGY. M. M. Tremblay[1,2], D. F. Mark[1,3], J. N. Carter[1], B. E. Cohen[1,2], A. Robinson[3], and P. Chung[2]. [1]Scottish Universities Environmental Research Centre (SUERC), Rankine Avenue, East Kilbride, G75 0QF, UK (marissa.tremblay@glasgow.ac.uk), [2]School of Geographical and Earth Sciences, The University of Glasgow, G12 8QQ, UK, [3]Department of Earth & Environmental Science, University of St Andrews, KY16 9AJ, UK.

Introduction: Application of the ^{40}Ar/^{39}Ar chronometer to lunar samples has significantly shaped our understanding of the inner Solar System's impact history [e.g., 1]. In particular, ^{40}Ar/^{39}Ar step-heating datasets from Apollo mission samples have provided the most widely cited evidence for a Late Heavy Bombardment (LHB) due to a clustering of apparent plateau ages at ~3.9 Ga [e.g., 2–4]. However, the analytical methods and interpretive approaches most commonly used for lunar ^{40}Ar/^{39}Ar datasets—and the consequent evidence for the LHB and for impact chronologies more generally—have recently been called into question [5–7].

Many lunar ^{40}Ar/^{39}Ar step-heating datasets exhibit evidence for partial resetting of the ^{40}Ar/^{39}Ar system, manifest as young initial step ages relative to apparent plateau ages observed in later steps [e.g., 8]. In these cases, the interpretation of plateau ages is inherently and systematically biased and may result in the identification of an apparent but false cluster of plateau ages [5]. One way to address this limitation is to quantitatively model the entire ^{40}Ar/^{39}Ar age spectra, rather than identify only an apparent plateau age [e.g., 8–9]. This requires the kinetics of argon diffusion in the K-bearing phase(s) present in a particular lunar sample to be known. To measure ^{40}Ar/^{39}Ar age spectra as well as argon diffusion kinetics, step-heating experiments must be carried out with precise temperature control and monitoring. Here, we present temperature-controlled ^{40}Ar/^{39}Ar step-heating experiments for a suite of lunar feldspathic breccias. We use sample-specific diffusion kinetics determined from each experiment to quantitatively model the time-temperature histories consistent with each ^{40}Ar/^{39}Ar age spectra.

Methods: We acquired material from 15 lunar meteorites of varying lithologies, including samples classified as fragmental breccias, impact melt breccias, and regolith breccias. We aimed to work with samples that, based on a comparison of their bulk elemental composition to Lunar Prospector gamma ray data [10], may sample regions of the lunar crust distinct from the Apollo mission samples (on which the vast majority of ^{40}Ar/^{39}Ar datasets have been collected). While some of the meteorites we are studying have existing ^{40}Ar/^{39}Ar age spectra but lack diffusion kinetic parameters, most have no previously reported ^{40}Ar/^{39}Ar data.

We initially examined each sample using Scanning Electron Microscopy (SEM) at the University of Glasgow Imaging Spectroscopy and Analysis Centre (ISAAC), obtaining large-area backscattered electron images and qualitative compositional maps by energy dispersive X-ray analysis. From this initial characterization, we selected individual lithic or impact melt clasts or impact melt regions in each breccia to sample for ^{40}Ar/^{39}Ar analyses. Following initial SEM analyses, we also used the Electron Microprobe Analysis Facility at the University of Edinburgh to obtain quantitative compositional information about the potential K-bearing phases in each sample. Since most clasts we selected for ^{40}Ar/^{39}Ar analyses were too small to subsample, we analyzed phases in petrographically and compositionally similar clasts by EPMA.

Selected clasts or impact melt regions were extracted and co-irradiated with the neutron fluence monitor standards Hb3gr and WA1ms [11–12] for 120 hours at the Oregon State University TRIGA rector in the CLICIT facility. Irradiated samples were placed inside platinum packets and baked under vacuum for ~48 hours. Temperatures during baking did not exceed 100 ºC, as monitored by a thermocouple inside of the sample chamber. Sample packets were then heated using a 75 W diode laser in a feedback control loop with an optical pyrometer, which we calibrated up to 1100 ºC using a K-type thermocouple to an accuracy of ± 6 ºC. Argon isotopes from each heating step were measured on an ARGUS V sector-field mass spectrometer using a 5-faraday collector array in the Argon Isotope Facility at SUERC. Experiments consisted of at least 30 and typically more than 40 heating steps and included at least one (and typically three) retrograde heating cycles. Experiments were completed when signal intensities of argon isotopes from a heating step were comparable to signal intensities measured in the subsequent background measurement.

To determine sample-specific diffusion kinetics, we use the fraction of ^{39}Ar released and the duration of each heating step to calculate diffusivities [13], assuming that the diffusion geometry is spherical and that the spatial distribution of ^{39}Ar is initially uniform in each diffusion domain. Essentially all of the clasts we selected contain multiple K-bearing phases (most commonly plagioclase and pyroxene, as well as K-bearing glass); therefore, the diffusivity we calculate for an individual heating step reflects a mixture of the argon diffusion kinetics of these different phases. Additionally, individual phases may be comprised of multiple diffusion domains [e.g., 14], which combined with the presence of multiple phases can lead to complex, highly nonlinear diffusion

behavior. To account for these samples' multiple phase, multiple diffusion domain nature and effectively model their argon diffusion kinetics, we are developing a Bayesian nonparametric model based on the multiple diffusion domain theoretical framework [14]. This modeling approach enables us to estimate the posterior probabilities of (1) the total number of diffusion domains present in a sample, and (2) the kinetic parameters of each domain. This approach produces similar results to recent work on multiphase lunar samples [e.g. 9, 15] but with less restrictive prior constraints and comprehensive uncertainty estimation.

With the modeled diffusion parameters for each sample, we solve for the production and diffusion of ^{40}Ar over geologic time as well as the laboratory degassing of ^{40}Ar and ^{39}Ar after ref. [15]. Initially, we explore thermal histories that involve only one reheating event, with the timing, duration, and peak temperature of the event allowed to be free model parameters. In the future, we plan to explore more complex models that allow for more than one reheating event.

Preliminary results: We will show ^{40}Ar/^{39}Ar datasets and thermal history model results for clasts from three lunar meteorites. Northwest Africa 482 is a very fine-grained impact melt breccia primarily consisting of plagioclase, pyroxene, and olivine, with isolated clasts of inherited plagioclase grains (Fig. 1A). Previous ^{40}Ar/^{39}Ar measurements reveal significant evidence for partial resetting, with a youngest initial step age < 1000 Ma, but also a complex age spectra with no apparent plateau [16]. Our initial ^{40}Ar/^{39}Ar age spectra is also complex and exhibits evidence for partial resetting, although our youngest initial step age is significantly older than previously reported. Northwest Africa 11444 is a polymict fragmental breccia for which no previous ^{40}Ar/^{39}Ar data exist. We sampled basaltic clasts from two different fragments of NWA 11444 (Fig. 1B). Rabt Sbayta 007 is also a polymict breccia containing abundant mineral and lithic clasts with a finer grained matrix. We sampled two gray-brown lithic clasts and one region of dark matrix. Ongoing analyses of clasts from both NWA 11444 and Rabt Sbayta 007 reveal highly disturbed and complex age spectra. Given these initial findings, we anticipate that our approach to modeling sample-specific diffusion kinetics and thermal histories will be essential for quantitatively interpreting the ^{40}Ar/^{39}Ar age spectra we generate for these meteorites.

Acknowledgements: This research was supported by the Royal Society Newton International Fellowship (#171365) and the Royal Astronomical Society Paneth Meteorite Trust Award. We are thankful to the following institutions and private collectors for providing sample material for analysis: Natural History Museum London, the Institute of Meteoritics at University of New Mexico, the Antarctic Meteorite Research at the Centre National Institute of Polar Research of Japan, Ben Hoefnagels and Graham Ensor. We also thank Chris Hayward with assistance collecting EPMA analyses.

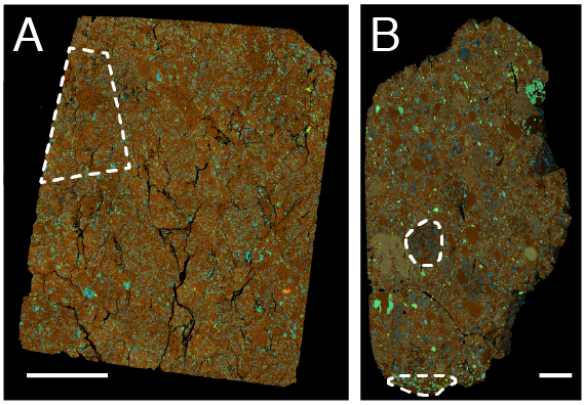

Figure 1. Backscattered electron images overlain with energy dispersive X-ray (EDX) maps of NWA 482 (A) and NWA 11444 (B). EDX mosaic is colored for aluminum (orange), magnesium (blue) and iron (green). The white dashed shapes denote regions or clasts selected for ^{40}Ar/^{39}Ar analyses. White scale bars are 1 mm long.

References: [1] Stoffler D. (2006) *Rev. Mineral. Geochem.*, *60(1)*, 519–596. [2] Dalrymple G. B. and Ryder G. (1993) *J. Geophys. Res.*, *98(E7)*, 13085–13095. [3] Dalrymple G. B. and Ryder G. (1996) *J. Geophys. Res. Planets*, *101(E11)*, 26069–26084. [4] Norman M.D. et al. (2006) *Geochim. Cosmochim. Acta*, *70(24)*, 6032–6049. [5] Boehnke P. and Harrison T. M. (2016) *Proc. Natl. Acad. Sci.*, *113(39)*, 10802–10806. [6] Boehnke P. et al. (2014) *LPS* XLV, Abstract #2545. [7] Harrison T.M. et al. (2018) *LPI Contrib.* 2107, Abstract #2031. [8] Shuster D. L. et al. (2010) *Earth & Planet. Sci. Lett.*, *290(1–2)*, 155–165. [9] Boehnke P. et al. (2016) *Earth & Planet. Sci. Lett.*, *453*, 267–275. [10] Calzada-Diaz A. et al. (2015) *Meteoritics & Planet. Sci.*, *50(2)*, 214–228. [11] Jourdan F. et al. (2006) *Chem. Geol.*, *231(3)*, 177–189. [12] Jourdan F. et al. (2014) *Geochim. Cosmochim. Acta*, *141*, 113–126. [13] Fechtig H. and Kalbitzer S. (1966) *Potassium Argon Dating*, 68-107. [14] Lovera O.M. et al. (1991) *J. Geophys. Res.*, *96(B2)*, 2057-2069. [15] Shuster D.L. and Cassata W.S. (2015) *Geochim. Cosmochim. Acta*, *155*, 154-171. [16] Daubar I.J. (2002) *Meteoritics & Planet. Sci.*, *37*, 1797-1813.